

المجلة الدولية للبحوث العلمية

Vol. (4), No. (7)

July 2025

الإصدار (4)، العدد (7)

Electrochemical Assessment of Thiazolidine Derivative as a Corrosion Suppressant for Carbon Steel in Acidic Medium

Asawer S. Temma*, Hanan M. Ali

Department of Chemistry, College of Education for Pure Sciences, University of Basrah, Basrah, Iraq
*asawer.tema@uobasrah.edu.iq

Abstract

A thiazolidine-based compound (AS₆) was synthesized and structurally confirmed through Fourier-transform infrared spectroscopy (FT-IR) and proton nuclear magnetic resonance (¹H-NMR) techniques. Its potential as a corrosion inhibitor for N80 carbon steel in a 1 M hydrochloric acid environment was systematically investigated. The study involved electrochemical assessments, adsorption modeling, activation energy calculations, and surface characterization using Tafel polarization, Langmuir isotherms, the Arrhenius approach, and scanning electron microscopy (SEM) coupled with energy-dispersive spectroscopy (EDS). The results revealed a notable enhancement in inhibition efficiency at elevated inhibitor concentrations, while higher temperatures led to a decline in performance. Tafel polarization data demonstrated a consistent reduction in corrosion rate as the inhibitor concentration increased. Surface analysis confirmed the development of a protective film on the steel substrate, highlighting the practical applicability of AS₆ in industrial corrosion mitigation.

Introduction

Metal corrosion has emerged as a significant concern across many industries worldwide, posing both economic and safety-related challenges. Corrosive damage



المجلة الدولية للبحوث العلمية

Vol. (4), No. (7)

July 2025

الإصدار (4)، العدد (7)

typically occurs when metallic materials interact with their surrounding environment, especially during industrial processes such as acid cleaning, pickling, and descaling [1]. Among these, corrosion is arguably one of the most frequent and undesirable phenomena, resulting from electrochemical reactions between the metal surface and aggressive media, ultimately compromising structural integrity [2].

In numerous industrial applications, acidic solutions are routinely employed to eliminate rust and scale deposits from steel surfaces. These solutions are also widely used in the petroleum sector to enhance hydrocarbon recovery through acid stimulation techniques. However, such operations frequently accelerate the degradation of steel pipes and processing equipment due to prolonged acid exposure [3].

The pressing need to address corrosion-related losses has driven extensive research into protective strategies, with corrosion inhibitors being among the most effective and practical approaches [4]. These inhibitors can act by targeting either anodic or cathodic reactions—or both—depending on their mechanism of interaction with the metal—solution interface. Their efficiency is often associated with the formation of a thin surface layer, which may result from adsorption, deposition, or passivation mechanisms [5].

Organic inhibitors, in particular, are known for forming protective films via adsorption onto metal surfaces [6]. Their performance is strongly influenced by the presence of electronegative atoms such as nitrogen, sulfur, and oxygen, as well as by the nature of their functional groups and the electron density at donor sites [7]. The inhibition process is governed by a range of physical, chemical, and electronic factors, including molecular structure, spatial configuration, and orbital interactions with the metal. Thiazolidine derivatives are a class of environmentally friendly compounds with broad applications in pharmaceuticals, food chemistry, and biomedicine. These compounds, especially those bearing additional heteroatoms like N and O along with aryl substituents, have shown promise as corrosion inhibitors in



المجلة الدولية للبحوث العلمية

Vol. (4), No. (7)

July 2025

الإصدار (4)، العدد (7)

aggressive environments. Their effectiveness arises from the presence of lone pair electrons and π -electron systems, which facilitate electron transfer and coordinate bond formation with unoccupied metal d-orbitals. The adsorption of these molecules is influenced by the metal's surface properties, the nature of the corrosive medium, and the chemical structure of the inhibitor [8] [1].

This study aims to contribute to the development of cost-effective and eco-friendly corrosion mitigation strategies by synthesizing a thiazolidine-based compound (AS₆) and evaluating its inhibition efficiency against the corrosion of N80 carbon steel in a 1 M hydrochloric acid solution.

Materials and Methods

The experimental work utilized high-purity reagents, including 4-chlorobenzaldehyde obtained from Merck and additional compounds supplied by Sigma-Aldrich, each with a certified purity of 99%. The metallic substrate employed was an N80 grade carbon steel alloy, cut into specimens with dimensions of 3 cm in length, 2 cm in width, and 0.2 cm in thickness.

Fourier-transform infrared (FT-IR) spectroscopy was conducted using a Shimadzu FT-IR 8400S spectrometer. Spectra were recorded in the range of 4000 to 500 cm⁻¹ using KBr pellet technique. Proton nuclear magnetic resonance (¹H NMR) spectra were obtained on a Bruker 500 MHz spectrometer, with tetramethylsilane (TMS) serving as the internal standard. The surface morphology of the steel samples was examined via scanning electron microscopy (SEM) using a TESCAN MIRA 3 FEG-SEM system. Hydrochloric acid served as the corrosive medium in this study and was diluted with deionized water to achieve the desired molar concentration of 1 M.

Carbon Steel Alloy Specification:

In this investigation, the carbon steel alloy N80 was employed as the metallic substrate. The alloy was sourced from the South Oil Company, and its elemental



المجلة الدولية للبحوث العلمية

Vol. (4), No. (7)

July 2025

الإصدار (4)، العدد (7)

composition is detailed in Table 1. The formulation reflects a standard industrial-grade carbon steel, with iron as the base element and minor additions of other alloying elements [9].

Table (1): Chemical Composition of N80 Carbon Steel Alloy

Element	Cr	Mn	Si	P	S	C	Fe
%	0.04	1.8	0.26	0.009	0.001	0.39	remained is Fe

Synthesis of Thiazolidine Derivative (AS_6):

The compound 2-(4-chlorophenyl) thiazolidine-4-carboxylic acid (AS₆) was synthesized by reacting 0.01 moles of L-cysteine with an equimolar amount (0.01 moles) of 4-chlorobenzaldehyde. The reaction was carried out in a 100 mL conical flask containing a solvent mixture of 50 mL ethanol and 10 mL distilled water. The mixture was stirred magnetically at ambient temperature for 12 hours.

Upon completion, the resulting precipitate was collected by filtration, washed thoroughly with diethyl ether, and left to air-dry. The crude product was subsequently recrystallized from a 1:3 ethanol-to-water mixture, yielding pure white crystals of the desired compound, as illustrated in the reaction scheme below [10].

CHO
$$+$$
 HS OH EtOH: H₂O $+$ HO $+$ NH₂ $+$ HO $+$ Cl $+$ Cl

Scheme (1): Preparation steps of Thiazolidine derivative (AS₆)

Preparation of AS₆ Inhibitor Concentrations:

A series of hydrochloric acid solutions with a fixed molarity of 1 M were prepared for the purpose of evaluating the electrochemical polarization behavior (Tafel analysis) of N80 carbon steel. Rectangular specimens of the alloy, with dimensions



المجلة الدولية للبحوث العلمية

Vol. (4), No. (7)

July 2025

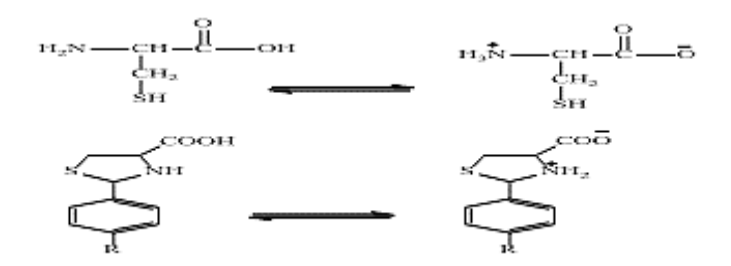
الإصدار (4)، العدد (7)

of 3 cm in length, 2 cm in width, and 0.2 cm in thickness, were immersed in solutions containing the corrosion inhibitor AS_6 at concentrations of 0.0001 M, 0.0005 M, 0.001 M, and 0.005 M, respectively.

Results and Discussion

FT-IR Spectral Analysis:

The FT-IR spectra of compound AS₆ reveal characteristic features indicative of its zwitterionic nature, as illustrated in Scheme 2. This spectral behavior closely resembles that of amino acids, where an internal equilibrium leads to the formation of a secondary ammonium salt group (+NH₂), which is observed as a broad absorption band spanning the range of 3500–2611 cm⁻¹. Additionally, the presence of carboxylate salt groups (COO⁻) is confirmed by two distinct absorption bands centered at 1581 cm⁻¹ and 1492 cm⁻¹, respectively [11].



Scheme (2): Zwitterionic structure of the compounds

Thiol (–SH) stretching vibration—confirms the successful cyclization of the thiazolidine ring. Furthermore, the disappearance of the aldehydic carbonyl (C=O) signal within the 1700–1750 cm⁻¹ region reinforces the completion of the synthesis.

Additional spectral features include a band near 3050 cm⁻¹ attributed to aromatic C–H stretching, while a peak around 2964 cm⁻¹ corresponds to aliphatic C–H stretching. The signal at 1492 cm⁻¹ is characteristic of C=C aromatic skeletal vibrations.

Thiazolidine ring-specific vibrations are also evident, with a strong absorption at 615



المجلة الدولية للبحوث العلمية

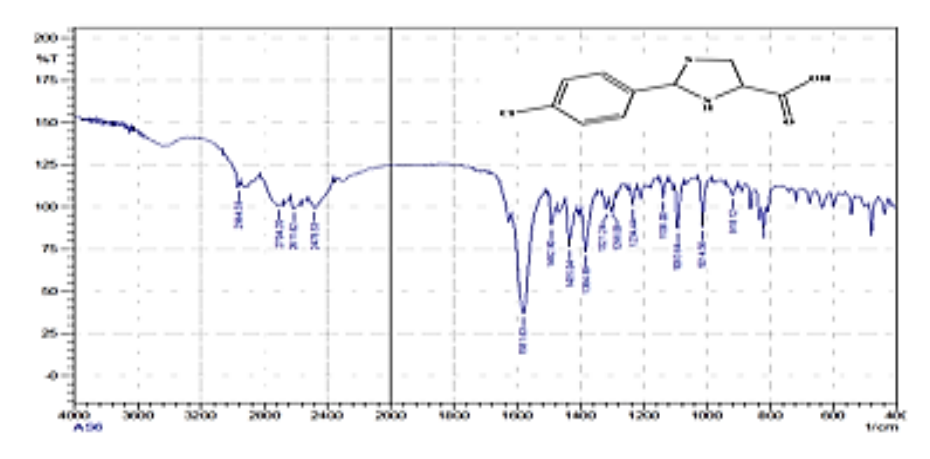
Vol. (4), No. (7)

July 2025

الإصدار (4)، العدد (7)

cm⁻¹ assigned to C–S stretching, a band within 1298–1321 cm⁻¹ corresponding to C–N stretching, and another at 1138 cm⁻¹ due to C–O stretching.

Furthermore, an increase in band intensity between 2500 and 1900 cm⁻¹ suggests the involvement of hydrogen bonding within the molecular structure. This is consistent with the behavior of thiazolidine-4-carboxylic acid derivatives, which often display intramolecular hydrogen bonding that influences the vibrational frequencies of OH and NH groups [12]. (Figure 1)



Figures (1): AS6 - FT-IR spectrum

¹H-NMR Analysis:

The ¹H-NMR spectrum of the synthesized compound in DMSO-d₆ revealed chemical shifts at approximately 2.5 ppm and 3.3 ppm for the solvent. A singlet was observed in the range of $\delta = 5.56-5.29$ ppm, attributable to the proton adjacent to the sulfur atom [H–C–S]. A triplet in the range of $\delta = 4.21-3.90$ ppm was assigned to the methylene protons adjacent to the carboxylic group [H–C–C=O], while the aromatic protons [H–Ar] appeared as a doublet between $\delta = 6.90-7.50$ ppm. Notably, signals corresponding to the carboxylic acid proton and the NH proton were absent in some instances, likely due to the compound's zwitterionic nature. This phenomenon is consistent with the internal charge stabilization typically observed in zwitterions



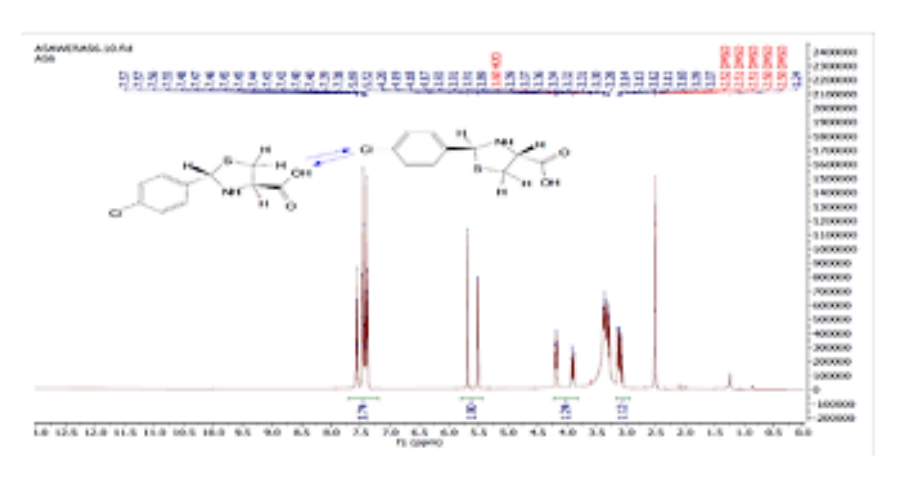
المجلة الدولية للبحوث العلمية

Vol. (4), No. (7)

July 2025

الإصدار (4)، العدد (7)

[13], as illustrated in Figure 2.



Figures (2): AS₆ - ¹HNMR spectrum

Polarization Curves [14]:

Polarization behavior was investigated in acidic environments consisting of 1 M hydrochloric acid solutions, using N80 carbon steel specimens both in the absence and presence of varying concentrations of the AS₆ inhibitor at different absolute temperatures. As depicted in Figures (3–6), an increase in the inhibitor concentration resulted in a noticeable shift in the corrosion potential (Ecorr) toward more positive values. However, no systematic trend was observed in the anodic and cathodic Tafel slopes. Additionally, a clear reduction in corrosion current densities (icorr) was detected as the inhibitor concentration increased. The inhibition efficiency (%IE) and surface coverage (Θ) also showed a positive correlation with inhibitor concentration. Conversely, raising the temperature at a fixed inhibitor concentration led to higher corrosion current densities and a corresponding decrease in inhibition efficiency [15].



المجلة الدولية للبحوث العلمية

Vol. (4), No. (7)

July 2025

الإصدار (4)، العدد (7)

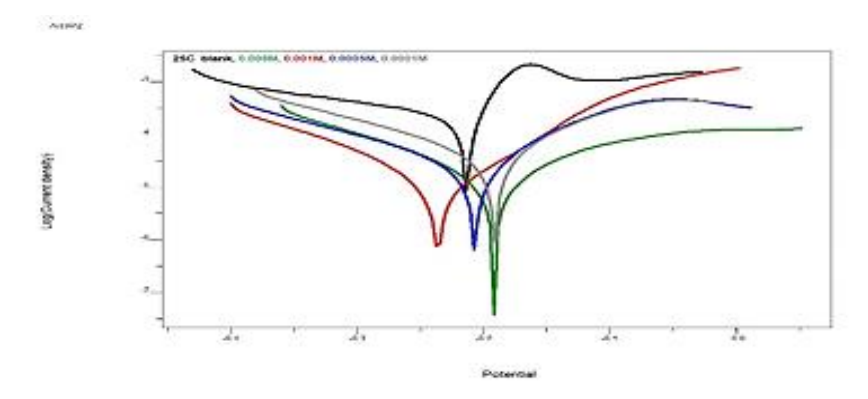


Figure (3): Tafel plot of carbon steel in the presence of AS₆ at (298K)

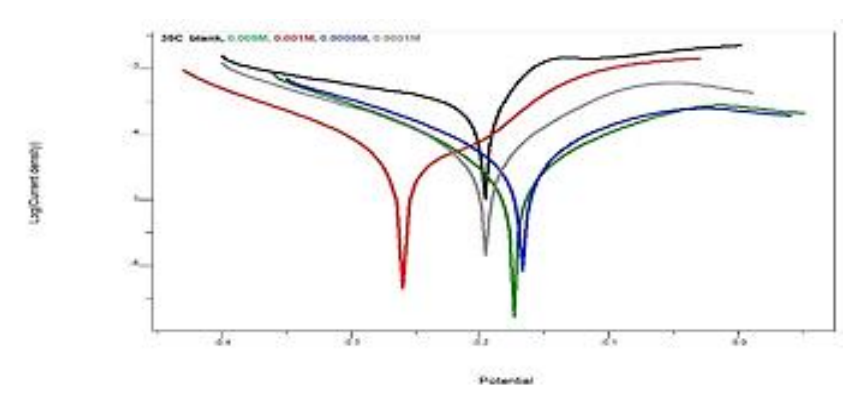


Figure (4): Tafel plot of carbon steel in the presence of AS₆ at (308K)

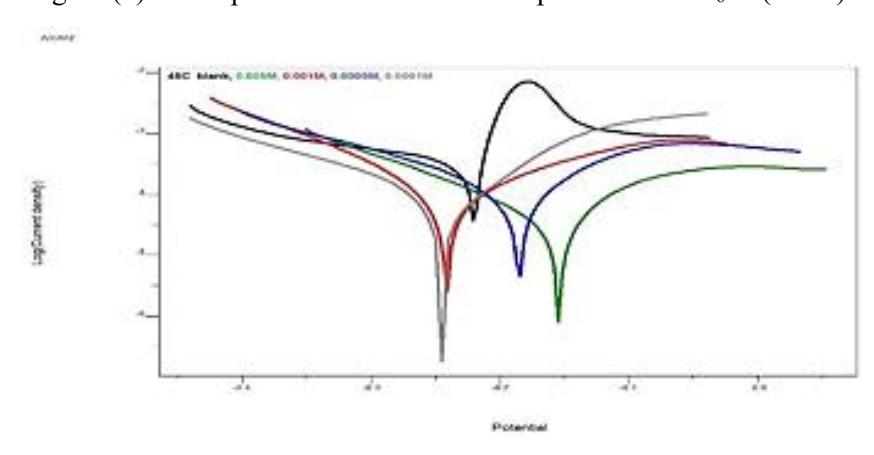


Figure (5): Tafel plot of carbon steel in the presence of AS₆ at (318K)



المجلة الدولية للبحوث العلمية

Vol. (4), No. (7)

July 2025

الإصدار (4)، العدد (7)

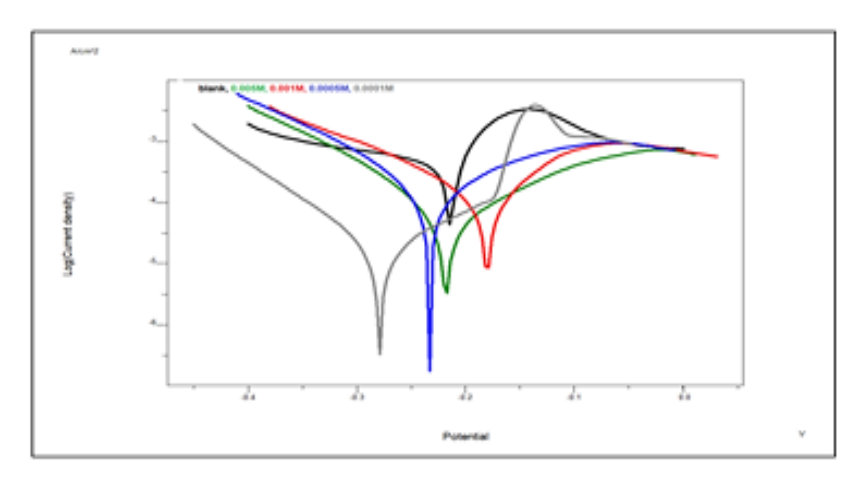


Figure (6): Tafel plot of carbon steel in the presence of AS₆ at (328K)

Table 1 provides quantitative data on the key electrochemical parameters, including corrosion current density (icorr), corrosion potential (Ecorr), anodic slope (βa), and cathodic slope (βc) derived from Tafel plots, in addition to inhibition efficiency (%IE) and surface coverage (θ). The results suggest that the dissolution of iron is effectively hindered in the presence of the AS₆ inhibitor, as evidenced by the decline in both anodic and cathodic current densities. This behavior is attributed to the formation of an adsorbed protective layer of AS₆ on the metal surface, which serves as a physical barrier against the aggressive acidic environment [16].

Table (1): Polarization data of N80 steel with AS₆ at different concentration and temperatures

Inhibitor Concentration	T (K)	-Ecorr (mV)	Icorr (mA/cm ²)	βc (mV/dec)	βα (mV/dec)	CR mpy	θ	IE%
	298	211.3	0.18610	275	32	0.0847686	-	-
Dlamle	308	193.7	0.25630	315	63	0.1167447	-	-
Blank	318	221.2	0.33020	355	21	0.1504061	-	-
	328	214.1	0.40330	345	55	0.1837032	-	-
	298	192.2	0.01443	113	121	0.0065729	0.92	92.25
0.005M	308	175.6	0.02241	113	128	0.0102078	0.91	91.26
0.005M	318	158.8	0.03415	119	100	0.0155553	0.89	89.65
	328	209.7	0.06588	104	141	0.0300083	0.83	83.66



المجلة الدولية للبحوث العلمية

Vol. (4), No. (7)

July 2025

الإصدار (4)، العدد (7)

	_	_	-	-			0	
Inhibitor	T	-Ecorr	Icorr	βc	βα	CR	θ	IE%
Concentration	(K)	(mV)	(mA/cm^2)	(mV/dec)	(mV/dec)	mpy		
	298	269.1	0.01871	114	128	0.0085224	0.89	89.94
0.001M	308	250.8	0.02784	100	113	0.0126811	0.89	89.13
0.001141	318	240.9	0.05206	108	159	0.0237133	0.84	84.23
	328	172.7	0.08393	138	86	0.0382301	0.79	79.19
	298	204.0	0.02427	162	90	0.011055	0.86	86.95
0 0005M	308	165.6	0.04419	135	119	0.0201285	0.82	82.76
0.0005M	318	181.4	0.06360	163	114	0.0289698	0.80	80.73
	328	230.2	0.13160	99	138	0.0599438	0.67	67.36
	298	197.4	0.02615	149	115	0.0119113	0.85	85.95
0.0001M	308	193.0	0.0619	142	97	0.0281955	0.75	75.85
0.0001M	318	232.1	0.07804	129	73	0.037064	0.76	76.36
	328	273.5	0.14520	85	105	0.0661386	0.63	63.99

Electrochemical polarization measurements revealed a noticeable decrease in both cathodic and anodic current densities as the inhibitor concentration increased. The findings indicate that the inhibition efficiency (%IE) improves proportionally with the rise in concentration. Surface coverage (θ) and the corresponding inhibition efficiency were calculated using Equations (1) [17]and (2) [18]respectively, to quantify the extent of protective film formation.

$$\theta = \left[i_{\text{corr.uninh}} - i_{\text{corr.inh}} / i_{\text{corr.uninh}}\right] \quad (1)$$

$$IE\% = \theta \times 100 \tag{2}$$

The collected data show that both the inhibition efficiency (%IE) and surface coverage (θ) consistently increased with higher inhibitor concentrations at all tested temperatures. This enhancement is attributed to the formation of a protective layer on the alloy's surface, whose thickness grows with concentration, thereby improving corrosion resistance [19], Fig. 7. However, a decline in %IE was observed at elevated temperaturesFig. 8, likely due to the desorption of the physically adsorbed layer. This behavior supports a physisorption mechanism occurring initially, followed by chemisorption at later stages [20]. The maximum inhibition efficiency, reaching 93.38%, was recorded at the optimal concentration of 0.005 M and a temperature of 298 K.

IJSR

المجلة الدولية للبحوث العلمية

Vol. (4), No. (7)

July 2025

الإصدار (4)، العدد (7)

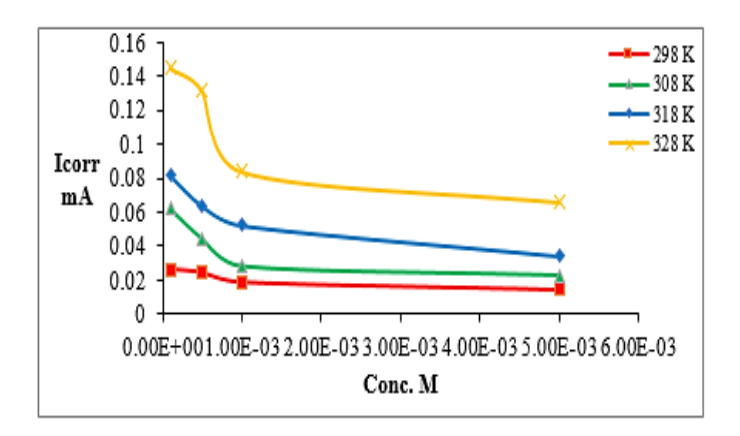


Figure (7): The effect of changing concentration on corrosion current density in acidic solutions with different inhibitor concentrations (AS₆) and for a range of temperatures (298-328K)

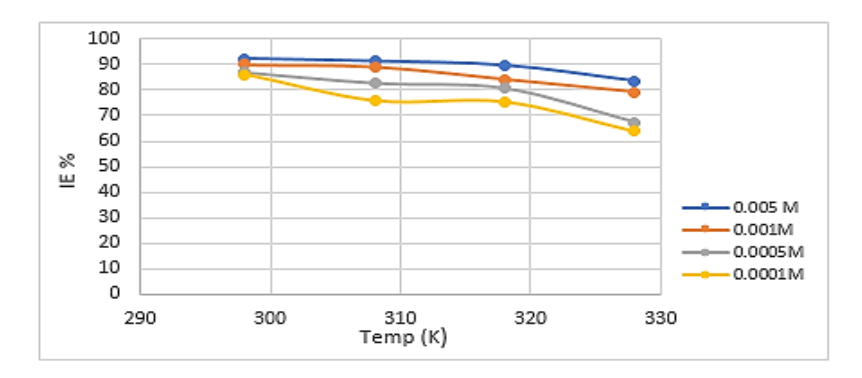


Figure (8): Effect of temperature on IE% at various concentrations of AS₆

Determination of Activation Energy (Ea):

The Arrhenius equation (Equation 3) was employed to evaluate the activation energy by plotting the logarithm of corrosion current density (log icorr) against the reciprocal of absolute temperature (1/T), as illustrated in Figure 9. The slope of the resulting straight line corresponds to –Ea/2.303R, from which the activation energy (Ea) is extracted:

$$Log icorr = Log A - E_a / (2.303RT)$$
 (3)



المجلة الدولية للبحوث العلمية

Vol. (4), No. (7)

July 2025

الإصدار (4)، العدد (7)

Here, icorr denotes the corrosion current density, A is the Arrhenius pre-exponential factor representing the frequency of molecular collisions, Ea refers to the activation energy, T is the absolute temperature, and R is the universal gas constant (8.314 J.mol⁻¹.K⁻¹). The linear relationship obtained from the plot confirms the validity of the Arrhenius model, with the slope reflecting the activation energy and the intercept corresponding to log A [21].

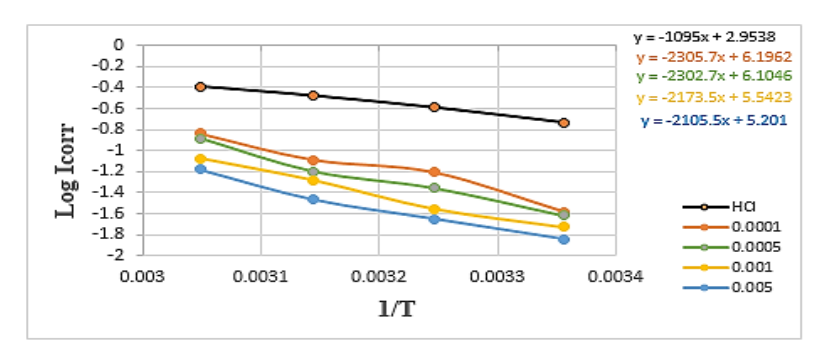


Figure (9): Arrhenius plots for N80 steel with and without AS₆ inhibitor at 298-328 K.

As shown in Table 2, the values of activation energy (Ea) for the corrosion process of carbon steel increase noticeably in the presence of the inhibitor when compared to the uninhibited condition. This elevation in Ea suggests the formation of an adsorbed inhibitor layer on the metal surface, which is primarily governed by physical (electrostatic) interactions [22][23]. This observation aligns well with the decline in inhibition efficiency at higher temperatures, which typically indicates a physisorption mechanism occurring initially, followed by the gradual emergence of chemisorption as the temperature increases [24].

Table (2): Activation energy (EA) and pre-exponential factor (A) values in the absence and with the Inhibitor

Comp.	Conc. (M)	$E_a(KJ.mol^{-1})$	A
HC1	1	20.967	899.00032
	0.0001	44.147	1571084.027
	0.0005	44.623	1272254.024
AS_6	0.001	45.717	348568.8308
	0.005	46.284	158863.8277



المجلة الدولية للبحوث العلمية

Vol. (4), No. (7)

July 2025

الإصدار (4)، العدد (7)

Adsorption Isotherm:

Values (θ) corresponding to various inhibitor concentrations. This approach aids in understanding the adsorption mechanism and corrosion inhibition behavior of the inhibitor molecules on N80 carbon steel surfaces. The displacement of pre-adsorbed water molecules from the metal surface is considered the initial step in which organic inhibitor molecules become adsorbed, as illustrated by the equation below.

$$Org_{(solu.)} + \chi H_2 O_{(ads)} \rightarrow Org_{(ads)} + \chi H_2 O_{(solu.)}$$

The analysis of adsorption isotherms provides critical insights into the interaction behavior between the inhibitor molecules and the metal surface, specifically interpreted through the application of the Langmuir adsorption model [25].

$$C/\theta = 1/K_{ads} + C \tag{3}$$

The variables C, θ , and K_{ads} represent the inhibitor concentration, surface coverage, and the equilibrium constant for the interaction between the metal and inhibitor, respectively. Figure 10 illustrates the Langmuir plot of the AS_6 inhibitor at various temperatures, depicting the relationship between C/θ and C, which yields a linear correlation. The resulting R^2 values, presented in Table 3, are close to 0.99, indicating a strong agreement with the Langmuir adsorption model. This high correlation reflects a uniform adsorption behavior among the inhibitor molecules and confirms the applicability of the Langmuir model in evaluating the adsorption equilibrium constant (K_{ads}).



المجلة الدولية للبحوث العلمية

Vol. (4), No. (7)

July 2025

الإصدار (4)، العدد (7)

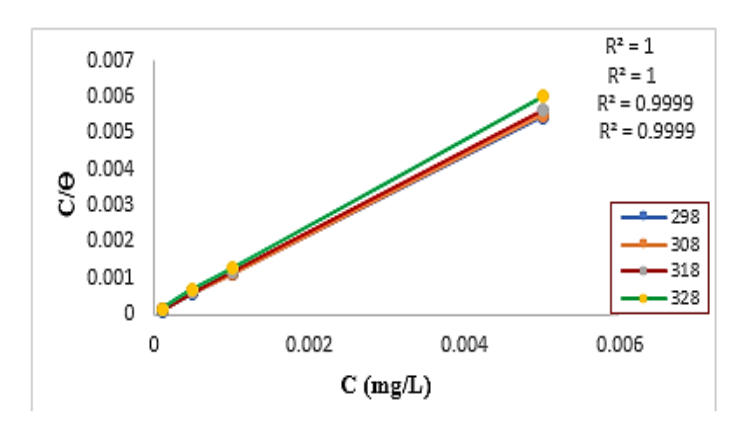


Figure (10): Langmuir adsorption isotherms (AS₆)

From the intercept value, the calculated K_{ads} is relatively high, indicating a strong adsorption affinity of the AS_6 inhibitor onto the carbon steel N80 surface. This elevated equilibrium constant suggests a substantial interaction between the inhibitor and the metal substrate. Based on the K_{ads} values, the standard Gibbs free energy [19] of adsorption (ΔG_{ads}°) was determined using Equation (4) below.

$$\Delta G^{\circ}_{ads} = -RT \ln (55.5 \times K_{ads})$$
 (4)

Here, R, T, and K represent the universal gas constant, absolute temperature, and adsorption equilibrium constant, respectively. The value 55.5 refers to the molar concentration of water molecules in the solution (mol/L). As shown in Table 3, the negative values of the Gibbs free energy (ΔG°_{ads}) suggest that the adsorption process

Table (3): Langmuir adsorption isotherm parameters for the adsorption of inhibitor (AS₆) onto the carbon steel surface at all investigated temperatures (298 to 328 K).

Comp.	Δ H _{ads} (kJ.mol ⁻¹)	Temp. K	R ²	\mathbf{K}_{ads}	Log K _{ads}	Δ G _{ads} (kJ.mol ⁻¹)	ΔS _{ads} (kJ.mol ⁻¹ .K ⁻¹)
		298	1	33779.203	4.528649	-35.78600939	0.037865
		308	1	24888.129	4.395992	-36.20470155	0.037995
AS_6	-24.5022	318	0.9999	18613.794	4.269835	-36.61217159	0.038082
		328	0.9999	13613.297	4.133963	-36.91034226	0.03783

Typically, values of ΔG°_{ads} [26] around –20 kJ/mol are indicative of physisorption,



المجلة الدولية للبحوث العلمية

Vol. (4), No. (7)

July 2025

الإصدار (4)، العدد (7)

whereas those equal to or more negative than -40~kJ/mol suggest chemisorption. The ΔG°_{ads} values obtained in this study point to a spontaneous physical adsorption process occurring on an energetically homogeneous surface. The observed decrease in ΔG°_{ads} at 328 K, along with its negative sign, confirms the spontaneity of the adsorption process and the stability of the adsorbed film on the carbon steel surface. The enthalpy of adsorption (ΔH°_{ads}) can be calculated using the Van't Hoff equation [20].

$$Log K_{ads} = (-\Delta H^{\circ}_{ads} / 2.303 RT) + Const$$
 (5)

By plotting Log K_{ads} against 1/T, a linear relationship with a negative slope is obtained, corresponding to $-\Delta H^{\circ}_{ads}/(2.303 \times R)$, as illustrated in Figure 11. The thermodynamic method also allows the estimation of the entropy of adsorption (ΔS°_{ads}) for the AS₆ inhibitor using Equation (6).

$$\Delta G^{\circ}_{ads} = \Delta H^{\circ}_{ads} - T\Delta S^{\circ}_{ads}$$
 (6)

Based on previous studies, a negative value of ΔH°_{ads} indicates that heat is released to the surroundings during the adsorption process, signifying an exothermic reaction. Conversely, a positive ΔH°_{ads} value implies that heat is absorbed from the environment into the system, indicating an endothermic reaction [27].

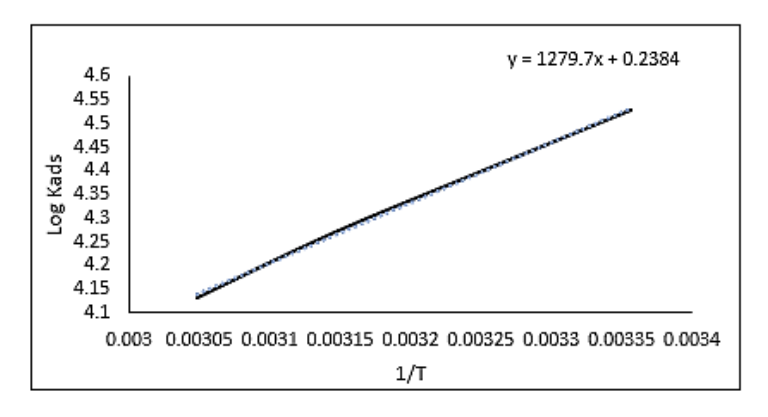


Figure (11): Correlation between $Log K_{ads}$ and 1/T for carbon steel N80 in a 1 M HCl solution with varying inhibitor concentrations of (AS₆)



المجلة الدولية للبحوث العلمية

Vol. (4), No. (7)

July 2025

الإصدار (4)، العدد (7)

The results indicate that the adsorption of the inhibitor is characterized by negative ΔH°_{ads} values, suggesting that the adsorption process is exothermic. This implies that the adsorption could be physical, chemical, or potentially a combination of both. Furthermore, the large and positive value of ΔS°_{ads} reflects an increase in disorder during the transition from the reactant to the adsorbed state, which enhances the adsorption on the metal surface.

Proposed Mechanism:

The mechanism of action for organic corrosion inhibitors [28] typically involves surface adsorption to form protective films that displace water molecules from the metallic surface, thereby shielding it from degradation. Adsorption is enhanced by heteroatoms such as nitrogen (N), oxygen (O), sulfur (S), or phosphorus (P), which possess lone pairs of electrons, in addition to π -electrons from multiple bonds or aromatic rings [29]. Chemisorption, in this context, refers to the process in which unshared electrons from the inhibitor molecule are transferred to or shared with the outer layer of the metal surface [30].

Organic inhibitors can adsorb onto metal surfaces via several interactions, including:

- Electrostatic attraction between charged atoms and the metal surface.
- Coordination between lone electron pairs and vacant d-orbitals of the metal.
- π -electron interactions between the inhibitor and the metal surface.

Key factors influencing the inhibitor's performance include the number of adsorption sites, charge density, molecular size, molecular orientation on the surface, and the inhibitor's ability to form insoluble metal—inhibitor complexes. The bonds formed between inhibitor molecules and the mild steel surface originate from the interaction of double-bond electrons or unshared electrons on oxygen and nitrogen atoms, which form chemical bonds with the outer metal layer [31], as illustrated in Figure (12).



المجلة الدولية للبحوث العلمية

Vol. (4), No. (7)

الإصدار (4)، العدد (7)

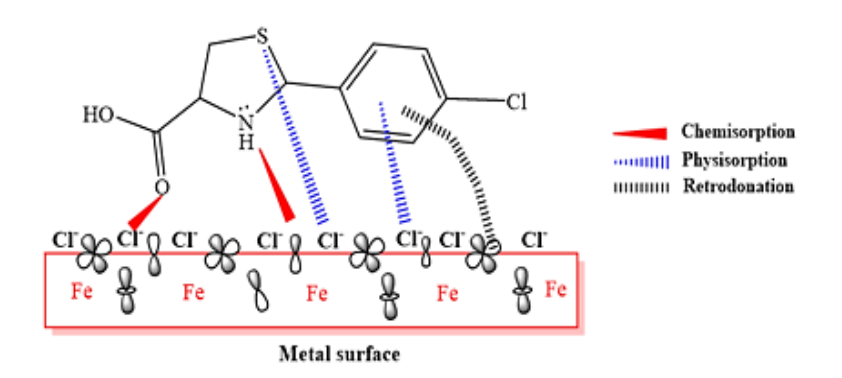


Figure (12): is a proposed mechanism for adsorption of the inhibitor on the metal surface

Scanning Electron Microscopy (SEM) and Energy-Dispersive X-ray Spectroscopy (EDS) Analysis [32] [33]:

Following immersion of AS₆ in 1 M hydrochloric acid solution for approximately 180 minutes, the surface morphology of the metal was examined using scanning electron microscopy (SEM). As shown in Figure 13(a), the corrosive action of the 1 M HCl solution resulted in surface roughness and visible defects on the mild steel surface. In contrast, Figure 13(b), corresponding to the AS₆-treated specimen, reveals a significantly smoother surface, free from pits or noticeable corrosion damage. This indicates that AS₆ effectively forms a protective barrier that shields the carbon steel surface from corrosive attack.

The study further aimed to identify the chemical constituents on the metal surface after exposure to 1 M HCl solution, with and without the presence of AS₆. Figures 14(a) and 14(b) present EDS spectra obtained from designated areas in the SEM images shown in Figures 13(a) and 13(b), respectively. From these measurements, the atomic ratios of elements present in the N80 carbon steel alloy were assessed following exposure to both the acidic environment and the inhibitor-containing solutions. The results show a notably higher oxygen content in the acid-only condition, whereas the oxygen signal was significantly reduced in the presence of



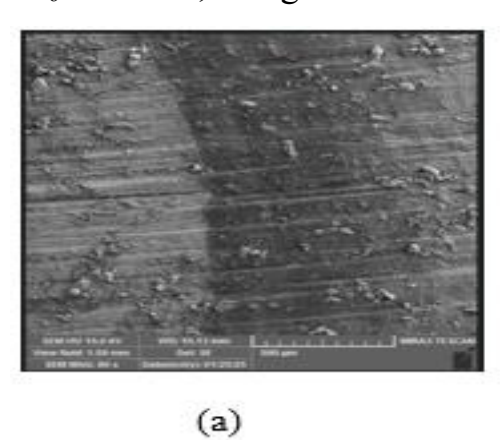
المجلة الدولية للبحوث العلمية

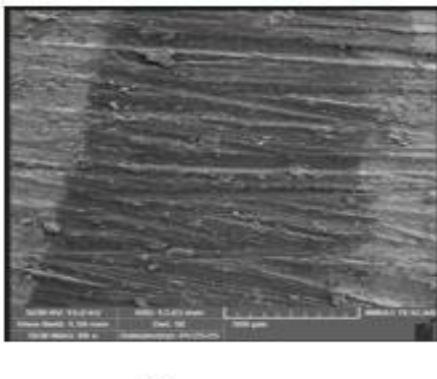
Vol. (4), No. (7)

July 2025

الإصدار (4)، العدد (7)

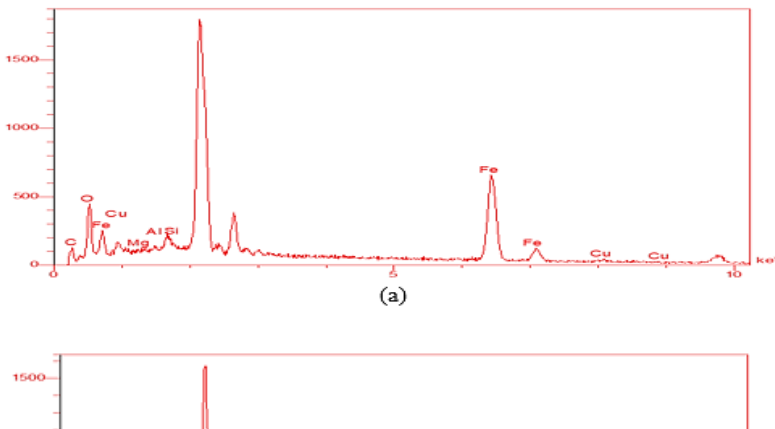
the AS₆ inhibitor, along with lower concentrations of other oxidizing species.





(b)

Figure (13): Photos for SEM of the mild steel N80 (a) after exposure to a 1 M HCl solution and (b) 1 M HCl solution containing 0.005 M of compound AS6



1000 Cu Aisi Cu Cu Aisi (b)

Figure (16): EDX spectra of N80 mild steel after exposure to different solution: (a) 1 M HCl alone, and (b) 1 M HCl containing 0.005 M of AS_6



المجلة الدولية للبحوث العلمية

Vol. (4), No. (7)

July 2025

الإصدار (4)، العدد (7)

Conclusions

The findings of this study demonstrate the effectiveness of compound AS₆ in mitigating the corrosion of carbon steel in an acidic medium. The maximum inhibition efficiency reached 92.25% at a concentration of 0.005 M and a temperature of 298 K, as determined by potentiodynamic polarization measurements. The adsorption behavior of AS₆ on the metal surface follows the Langmuir isotherm model, indicating a mixed-type adsorption mechanism. This was supported by thermodynamic evaluations and adsorption isotherm analyses. Furthermore, surface morphology analysis and EDS spectroscopy confirm that the inhibition activity of AS₆ arises from its adsorption onto the metal surface, forming a protective layer that hinders corrosion.

References

- 1. R. S. Ghada S. Masaret, "Synthesis and evaluation of a novel pyridinyl thiazolidine derivative as an antioxidant and corrosion inhibitor for mild steel in acidic environments," Arabian Journal of Chemistry, vol. 17, no. 6, Jun. 2024.
- 2. A. Sultan, S. H. Ali, and A. Nabi, "Synthesis, Identification and Inhibition Evaluation of Azo Dyes for Corrosion of Carbon-Steel Alloy In Acidic Medium: Thermodynamic and Kinetic Aspects", [Online]. Available: https://www.researchgate.net/publication/366167565.
- 3. Z. K. Kuraimid, D. S. Abid, and A. E. A. S. Fouda, "Synthesis and Characterization of a Novel Quaternary Ammonium Salt as a Corrosion Inhibitor for Oil-Well Acidizing Processes," ACS Omega, vol. 8, no. 30, pp. 27079–27091, Aug. 2023, doi: 10.1021/acsomega.3c02094.
- 4. Ashraqt Ahmeda*Adnan Sultanb, "Synthesis Characterization and DFT Studies of New Azo Dye Derived from Dapsone and Evaluation it as Corrosion Inhibiter," Forest Chemicals Review, pp. 1431–1449, Sep. 2022.
- 5. R. A. b, A. K. a, M. A. H. a, N. Y. T. a Khalid A. Alamry a, "Evaluation of corrosion inhibition performance of thiazolidine-2, 4-diones and its amino derivative: Gravimetric, electrochemical, spectroscopic, and surface morphological studies," Process Safety and



المجلة الدولية للبحوث العلمية

Vol. (4), No. (7)

July 2025

الإصدار (4)، العدد (7)

Environmental Protection, vol. 159, pp. 178–197, Mar. 2022.

- 6. H. Thamer Obaid, M. Yousif Kadhum, and A. Sultan Abdulnabi, "Quantum Chemical Calculations and Experimental Studies of using Azo Dye as Corrosion Inhibitors for on Carbon Steel in Acidic Medium."
- 7. R. Solmaz, M. E. Mert, G. Kardaş, B. Yazici, and M. Erbil, "Online English edition of the Chinese language journal Cite this article as," 2008. [Online]. Available: www.whxb.pku.edu.cn.
- 8. B. A. A. J. Ghada S. Masaret, "Inhibitive and adsorption behavior of new thiazoldinone derivative as a corrosion inhibitor at mild steel/electrolyte interface: Experimental and theoretical studies," J Mol Liq, vol. 338, 2021.
- 9. G. Palumbo, K. Kollbek, R. Wirecka, A. Bernasik, and M. Górny, "Effect of CO2 partial pressure on the corrosion inhibition of N80 carbon steel by gum arabic in a CO2-water saline environment for shale oil and gas industry," Materials, vol. 13, no. 19, Oct. 2020, doi: 10.3390/MA13194245.
- 10. A. A. Majed and D. Abid, "Synthesis, Characterization and Biological Activity Study of some New Thiazolidine Derivatives," 2015. [Online]. Available: https://www.researchgate.net/publication/349217250.
- 11. T. E. J. & A. M. J. W. A. Radhi, "An Eco-Friendly Ultrasound-Assisted Synthesis of a New Poly (thiourea-amide) and Its Application in the Removal of Ni(II) Ions from an Aqueous Solution," Russian Journal of General Chemistry, vol. 94, pp. 2382–2391, 2024.
- 12. S. P. P. U. (formerly U. of P. P. I. M. A. R. Y. B. D. & Satish K. P. Rohidas M. JagtapDepartment of Chemistry, "Crystal structure, computational studies, and stereoselectivity in the synthesis of 2-aryl-thiazolidine-4-carboxylic acids via in situ imine intermediate," Journal of Sulfur Chemistry, vol. 37, no. 4, pp. 401–425, Mar. 2016.
- 13. Q. R. A. H. H. A.-H. D. S. A. A. A. A. A. A. A. A. E. Ahmed A. Majed, "Synthesis, Characterization, Bioactivity Evaluation, and POM/DFT/Docking Analysis of Novel Thiazolidine Derivatives as Potent Anticancer and Antifungal Agents," CHEMISTRY EUROP, vol. 9, no. 40, Oct. 2024.
- 14. X. H. Y. Z. Y. S. X. M. H. G. Y. Z. Fang Ge, "Corrosion Behavior of 2205 DSS Base Metal



المجلة الدولية للبحوث العلمية

Vol. (4), No. (7)

July 2025

الإصدار (4)، العدد (7)

and ER 2209 Weld Metal in a Deposited Ash/Water Suspension," Int J Electrochem Sci, vol. 16, no. 7, 2021.

- 15. A. M. Jabbar and A. S. Abdulnabi, "Corrosion inhibitors for carbon steel N80 in an acidic medium by using the compound (E)-N-(benzo[d]thiazol-2-yl)-1-(2,3-dihydrobenzo[b][1,4]dioxin-6-yl)methanimine," International Journal of Corrosion and Scale Inhibition, vol. 13, no. 2, pp. 1146–1163, 2024, doi: 10.17675/2305-6894-2024-13-2-27.
- 16. Z. Sharifi, M. Pakshir, A. Amini, and R. Rafiei, "Hybrid graphene oxide decoration and water-based polymers for mild steel surface protection in saline environment," Journal of Industrial and Engineering Chemistry, vol. 74, pp. 41–54, Jun. 2019, doi: 10.1016/j.jiec.2019.01.043.
- 17. S. A. a, H. H. b c, T. D. b, M. A.-N. d e, N. G. f Abdelkader Ziouani a, "Molecular dynamic simulation and experimental investigation on the synergistic mechanism and synergistic effect of (1Z) N [2 (methylthio) phenyl] 20x0propanehydrazonoyl chloride corrosion inhibitor on mild steel in acid medium1M HCl," vol. 100, no. 1, p. 100832, Jan. 2023.
- 18. M. H. Raheema, N. A. Khudhair, T. H. AL-Noor, S. R. Al-Ayash, H. H. Kharnoob, and S. M. H. Obed, "Enhancement of corrosion protection of metal carbon steel C45 and stainless steel 316 by using inhibitor (Schiff base) in sea water," Baghdad Science Journal, vol. 20, no. 3, pp. 1012–1026, 2023, doi: 10.21123/bsj.2023.7749.
- 19. M. J. B. T. A.-G. C. A. G. & M. V. M. Saviour A. Umoren, "Inhibition of mild steel corrosion in HCl solution using chitosan," vol. 20, pp. 2529–2545, Aug. 2013.
- 20. S. K. Ahmed, W. B. Ali, and A. A. Khadom, "Synthesis and investigations of heterocyclic compounds as corrosion inhibitors for mild steel in hydrochloric acid," International Journal of Industrial Chemistry, vol. 10, no. 2, pp. 159–173, Jun. 2019, doi: 10.1007/s40090-019-0181-8.
- 21. O. A. Akinbulumo, O. J. Odejobi, and E. L. Odekanle, "Thermodynamics and adsorption study of the corrosion inhibition of mild steel by Euphorbia heterophylla L. extract in 1.5 M HCl," Results in Materials, vol. 5, Mar. 2020, doi: 10.1016/j.rinma.2020.100074.
- 22. A. B. T. Szauer, "Adsorption of oleates of various amines on iron in acidic solution," Electrochim Acta, vol. 26, no. 9, pp. 1253–1256, Sep. 1981.



المجلة الدولية للبحوث العلمية

Vol. (4), No. (7)

July 2025

الإصدار (4)، العدد (7)

- 23. A.S. FoudaCorresponding Author; M. Abdallah; A.M. Atya; H.D. Sabaa, "Corrosion Inhibition of Copper in Nitric Acid Solution Using Some Secondary Amines," The Journal of Science & Engineering, pp. 610–619, May 2012.
- 24. H. H. a, D. D. a b, M. A.-N. c, S. C. a Tahar Douadi a, "Effect of temperature and hydrodynamic conditions on corrosion inhibition of an azomethine compounds for mild steel in 1 M HCl solution," J Taiwan Inst Chem Eng, vol. 71, pp. 388–404, Feb. 2017.
- 25. A. Kokalj, "On the use of the Langmuir and other adsorption isotherms in corrosion inhibition," Corros Sci, vol. 217, Jun. 2023, doi: 10.1016/j.corsci.2023.111112.
- 26. A. Kadhim et al., "A mini review on corrosion, inhibitors and mechanism types of mild steel inhibition in an acidic environment," 2021, Russian Association of Corrosion Engineers. doi: 10.17675/2305-6894-2021-10-3-2.
- 27. T. D. S. I. S. C. Djamel Daoud, "Adsorption and corrosion inhibition of new synthesized thiophene Schiff base on mild steel X52 in HCl and H2SO4 solutions," Corros Sci, vol. 79, pp. 50–58, Feb. 2014.
- 28. M. Şahin, S. Bilgiç, and G. Gece, "Inhibition of armco iron corrosion in 1 m hcl medium using saponin: Experimental and computational studies," International Journal of Corrosion and Scale Inhibition, vol. 9, no. 4, pp. 1444–1458, 2020, doi: 10.17675/2305-6894-2020-9-4-16.
- 29. a W. D. and S. Z. Lei Guo, "Theoretical challenges in understanding the inhibition mechanism of copper corrosion in acid media in the presence of three triazole derivatives," Royal Society of CHEMISTRY, no. 79, 2014.
- 30. L. Guo, C. Qi, X. Zheng, R. Zhang, X. Shen, and S. Kaya, "Toward understanding the adsorption mechanism of large size organic corrosion inhibitors on an Fe(110) surface using the DFTB method," RSC Adv, vol. 7, no. 46, pp. 29042–29050, 2017, doi: 10.1039/c7ra04120a.
- 31. K. A. Alamry, M. A. Hussein, A. Musa, K. Haruna, and T. A. Saleh, "The inhibition performance of a novel benzenesulfonamide-based benzoxazine compound in the corrosion of X60 carbon steel in an acidizing environment," RSC Adv, vol. 11, no. 12, pp. 7078–7095, Feb. 2021, doi: 10.1039/d0ra10317a.



المجلة الدولية للبحوث العلمية

Vol. (4), No. (7)

July 2025

الإصدار (4)، العدد (7)

- 32. Z. Belarbi; F. Farelas; D. Young; M. Singer; S. Nesic, "Effect of Operating Parameters on the Inhibition Efficacy of Decanethiol," CORROSION, Apr. 2018.
- 33. T. Yu, F. Zhang, L. Zhao, X. Lu, and S. Xie, "Crack Failure Analysis of Stainless Steel Seamless Pipe," in Advances in Transdisciplinary Engineering, IOS Press BV, Oct. 2023, pp. 98–103. doi: 10.3233/ATDE230446.